Quantification and Qualitative Effects of Different PEGylations on Poly(butyl cyanoacrylate) Nanoparticles

Andreas K.O. Åslund[1,], Einar Sulheim[1,2,*], Sofie Snipstad[1], Eva von Haartman[3], Habib Baghirov[1], Nichola Starr[4], Mia Kvåle Løvmo[1], Sylvie Lelú[1], David Scurr[4], Catharina de Lange Davies[1], Ruth Schmid[2], Ýrr Mørch[2]*

AUTHOR ADDRESS

1. Department of Physics, Norwegian University of Science and Technology (NTNU), Trondheim, Norway
2. SINTEF Materials and Chemistry, Trondheim Norway
3. Pharmaceutical Sciences Laboratory, Åbo Akademi University, Turku, Finland
4. School of Pharmacy, The University of Nottingham, United Kingdom, NG7 2RD

*Authors contributed equally

Corresponding author: AÅ, andreas.aslund@ntnu.no, andreas.aaslund@gmail.com

ABSTRACT

Protein adsorption on nanoparticles (NPs) used in nanomedicine leads to opsonization and activation of the complement system in blood, which substantially reduces the blood circulation time of NPs. The most commonly used method to avoid protein adsorption, is to coat the NPs with polyethylene glycol, so called PEGylation. Although PEGylation is of utmost importance for designing the *in vivo* behavior of the NP, there is still a considerable lack of methods for characterization and fundamental understanding related to the PEGylation of NPs. In this work we

have studied four different poly(butyl cyanoacrylate) (PBCA) NPs , PEGylated with different types of PEG-based non-ionic surfactants – Jeffamine M-2070, Brij L23, Kolliphor HS 15, Pluronic F68 – or combinations thereof. We evaluated the PEGylation, both quantitatively by nuclear magnetic resonance (NMR), thermogravimetric analysis (TGA) and time-of-flight secondary ion mass spectrometry (ToF-SIMS), and qualitatively by studying ζ-potential, protein adsorption, diffusion, cellular interactions and blood circulation half-life. We found that NMR and ToF-SIMS are complementary methods, while TGA is less suitable to quantitate PEG on polymeric NPs. It was found that longer PEG increases both blood circulation time and diffusion of NPs in collagen gels.
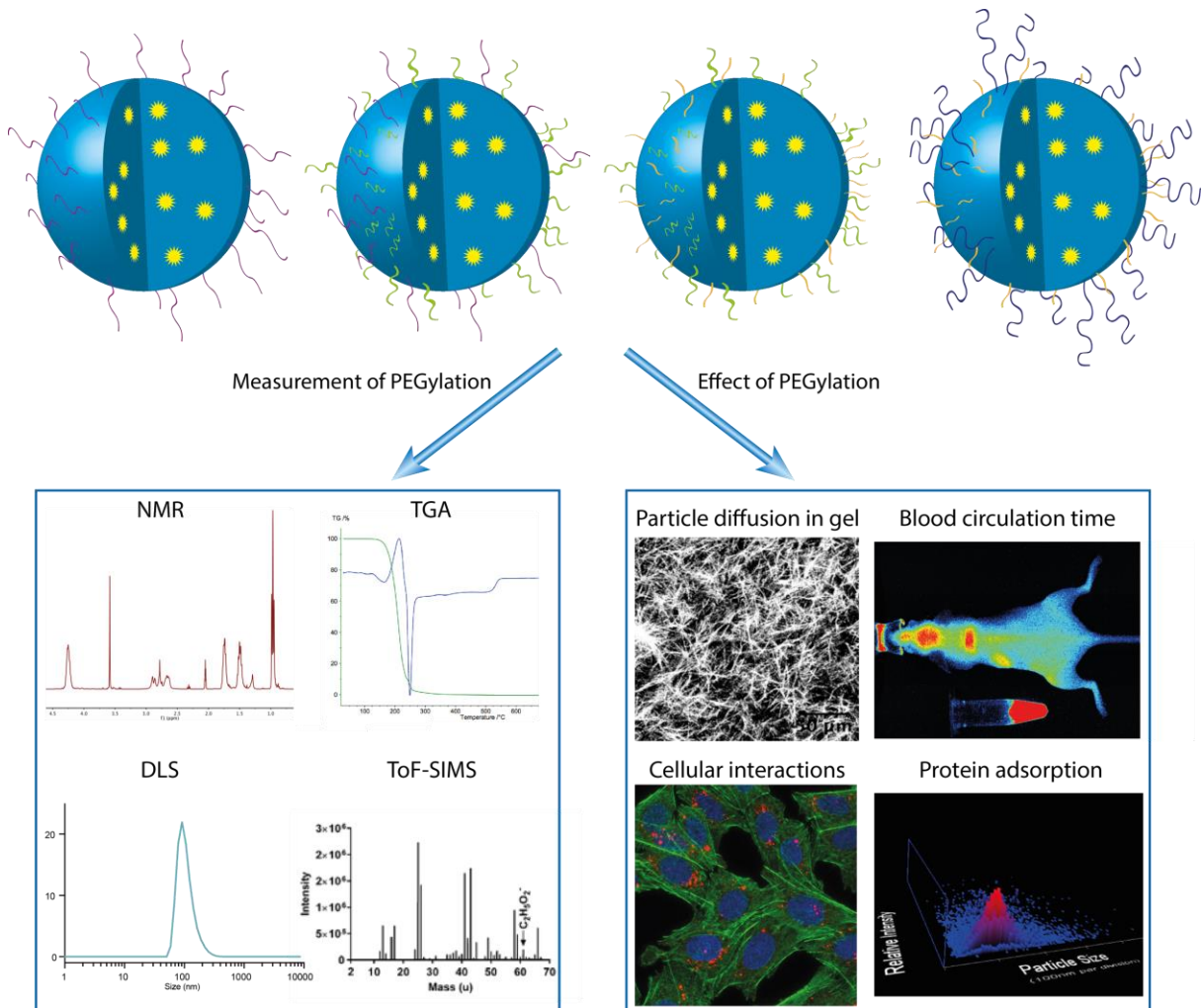
Introduction

Nanoparticles (NPs) in drug delivery have obtained large interest and are heavily investigated.[1] Most NP drug delivery systems aim to improve cancer therapy by exploiting the enhanced permeability and retention effect (EPR) and use active targeting or external stimuli to increase specificity compared to conventional cytostatic drugs.[2-6] EPR is the result of poorly developed vasculature being permeable to macromolecules and NPs and a lack of lymphatic drainage which together result in increased uptake and retention of the NPs in cancer tissue.[7] Active targeting can be achieved by conjugating receptor targets on the NP surface to enhance NP uptake and accumulation in specific cells.[8] External stimuli can be achieved by the NP being heat sensitive and by increasing the temperature in the target tissue, drug release is initiated.[9] A common denominator for NP drug delivery is that the NPs must avoid the immediate clearance by the immune system to have sufficient blood circulation time.[10] To achieve this, their surface is very often coated with PEG [poly(ethylene glycol)], which creates a water corona around the NP.[11] Depending on the density of PEG on the surface, the PEG is classified as being in a brush or mushroom conformation.[12] PEG can stabilize the NPs and reduce opsonization and activation of the complement system in blood and reticuloendothelial systems in liver, spleen and kidneys.[11] The PEGylation can be performed either during or post synthesis of the NPs, by either a covalent or non-covalent bond, resulting in varying properties of the PEGylation. However, evaluation of the PEGylation is often challenging and time consuming due to the importance of orientation and concentration for the function of PEG. The consequence of limited assessment of PEGylation is that the direct effects of PEG on blood circulation half-life, NP degradation, tissue accumulation and cellular uptake become uncertain.

Poly(alkyl cyanoacrylate) (PACA) NPs are well suited for drug delivery due to high drug loading capacity, ease of fabrication and controllable degradation at physiological conditions.[13-14] Although PACA NPs are rather well characterized, there is, to our knowledge, only one study describing the direct relationship between PEG length and their physicochemical *in vitro* and *in vivo* properties.[15]

In the present work we have synthesized PBCA [poly(butyl cyanoacrylate)] NPs PEGylated with different combinations of PEGs, to study how PEGylation can be quantified and how PEGylation affects the NPs in different *in vitro* and *in vivo* models. The PEGylation was analyzed by NMR (nuclear magnetic resonance), TGA (thermogravimetric analysis) and ToF-SIMS (Time-of-Flight Secondary Ion Mass Spectrometry). NMR and TGA are both quantitative methods that measure the PEGylation in bulk. ToF-SIMS is a semi-quantitative, mass spectrometry-based method that analyses the PEG available at the surface of a dried sample. In this study, the qualitative effects of PEGylation were evaluated by measuring the ζ-potential of the NPs, protein adsorption in the presence of bovine serum albumin (BSA) and rat serum, diffusion in an extracellular matrix (ECM) model, cellular uptake in macrophages and blood circulation time in mice. Although the current work is based on PBCA NPs, the methods and partly conclusions can be extended to other PEGylated systems such as other polymeric NPs, liposomes, lipid nanoparticles and nanoemulsions.

Experimental

NP Synthesis: Chemicals were purchased from Sigma Aldrich (St. Louis) and used as is unless otherwise specified. To evaluate the effect of PEGylation, PBCA NPs were produced in one step

using miniemulsion polymerization as previously described.[16] Briefly, an oil-in-water emulsion was prepared by mixing a monomer oil phase with a water phase (0.1M HCl) containing two of the surfactants:: Brij® L23 (tricosaethylene glycol dodecyl ether, **Brij**, 5mM), Pluronic® F68 (polyoxyethylene-polyoxypropylene block copolymer, **Plu**, 2.5mM), Kolliphor® HS 15 (Polyethylene glycol (15)-hydroxystearate, **Kol**, 5mM), Sodium dodecyl sulphate (**SDS**, 30mM) and Jeffamine® M-2070 (polyoxyethylene-polyoxypropylene-polyoxyethylene amine block copolymer, **JA**, 30mM, kindly provided by Huntsman Corporation). Four different combinations of surfactants were used: JA/SDS, JA/Brij, Kol/Brij and Kol/Plu. SDS is an anionic stabilizer while JA, Brij, Kol and Plu are non-ionic amphiphilic PEGs of different chain length (Fig. 1). The monomer phase contained butyl cyanoacrylate (BCA, kindly provided by Henkel Loctite), as well as a neutral oil as co-stabilizer (Miglyol®810N, 2wt%, Cremer), a radical initiator (V65, Azobisdimetyl valeronitril, Wako, 0.9wt%) and 0.2wt% of the fluorescent dye NR668 (modified Nile Red,[17-18] a kind gift from Dr. Klymchenko, University of Strasbourg). An oil-in-water nanoemulsion was achieved by sonification (ultrasonifier, Branson). JA and Kol act both as PEG and initiators as they contain a hydrophobic chain with a reactive amine (JA) or hydroxyl (Kol) group which initiate polymerization at the droplet surface. In the case where JA was used, it was added right after sonication to avoid premature polymerization. Polymerization was carried out at ambient temperatures overnight. Potential unreacted monomer in the particle core was polymerized by increasing the temperature to 50 °C for 8 h, activating free radical polymerization by V65. Excess PEG was removed by extensive dialysis against 1 mM HCl.
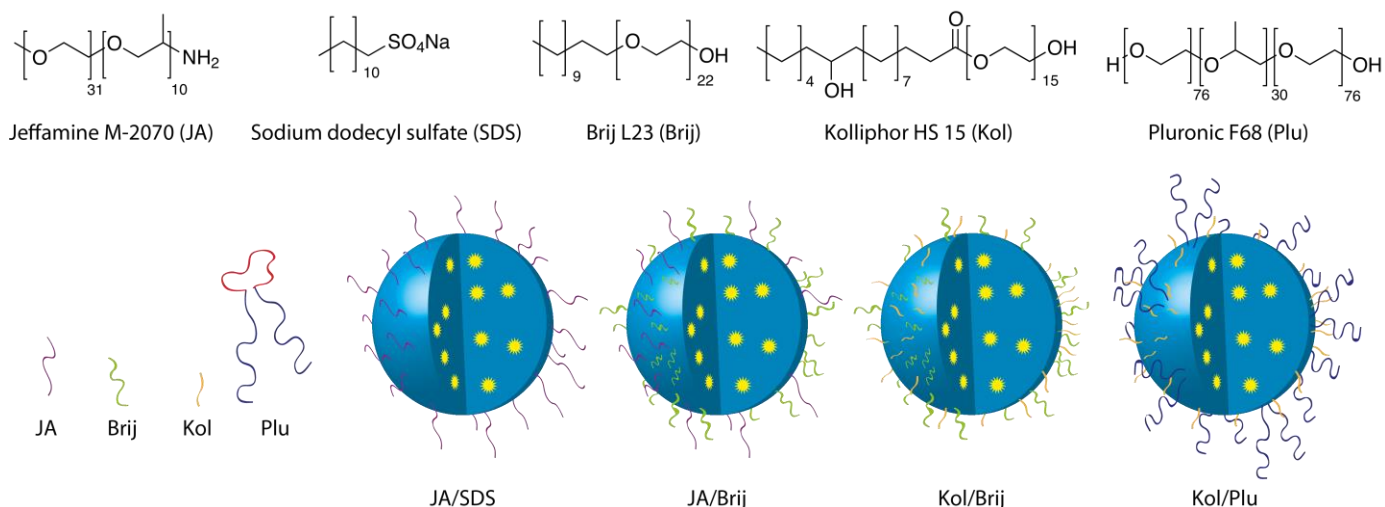
Fig. 1: Top row: structures of the different surfactants used in the study. Bottom row: schematic representation of the different NPs and their PEGylation pattern.

Dynamic (and Electrophoretic) Light Scattering (DLS): The size, size distribution and ζ-potential were determined using dynamic and electrophoretic light scattering (Zetasizer Nano ZS, Malvern Instruments) in 0.01M phosphate buffer, pH 7. The reported size is the Z-average.

NMR: PEGylation of the NPs was quantified by [1]H-nuclear magnetic resonance (NMR) using a 400 (400.13) MHz Bruker Avance DPX with autosampler (parameters: zg30 pulse sequence, 30° pulse, 1 s delay time, 32 scans, 65536 points spectral width, 3.96 min acquisition time). Preceding NMR, the dialyzed NPs were washed with deionized water (DIW) and centrifuged 3 times before drying at 50°C for 12-18 h. The sample was dissolved in Acetone-D_6. The spectra were processed using Mestrenova 9.0.1 (Mestrelab Research S.L.) using an exponential window function (0.30 Hz). The solvent residual peak for Acetone at 2.05 ppm was used as reference.[19] To calculate the PEGylation, the characteristic PEG-peaks at 3.6 ppm, the peak of a triplet from Miglyol 810N at 2.33 ppm and methylene group of PBCA at 1.75 ppm[20] and were integrated (See supplementary

Fig. 1 and 2 for example spectra and reference spectra). From these integrals, number of protons corresponding to each integral, and prior knowledge about the dry weight of the material and the size (Z-average), concentration and density (1.148 g/mL)[21] of the NPs, the number of ethylene units/nm^2 could be calculated (Supplementary Equations 1-14 and Supplementary Table 1). The molar ratio between JA and Brij was also quantified by using a unique proton at 3.29 ppm from JA (Inset Supplementary Fig. 1). It was not possible to calculate the molar ratio of the two PEG-surfactants in NPs with Kol/Brij or Kol/Plu as no fingerprint peaks were available.

TGA-DSC: Combined Thermogravimetric analysis (TGA) and Differential Scanning Calorimetry (DSC) (STA 449 F1 Jupiter®) was used to determine the amount of PEG grafted onto the NPs as wt% of the total NP mass. Approximately 10 mg of dry sample was weighed up in Al$_2$O$_3$ crucibles and subjected to a heating program in the temperature interval 35–900°C, with a constant heating rate 10 K/min, under synthetic air atmosphere. Results were recorded as change in weight loss (%) (TGA)/heat flow (µV) (DSC) over time and temperature increase. The mass changes (%) of the samples were analyzed with the Netzsch Proteus® Software.

ToF-SIMS: Following a 1/250 dilution in DIW, a small volume of each sample (<10 µL) was spotted onto a silicon wafer. The samples were then dried in a vacuum oven at 40°C for 30 min prior to analysis. Analysis was conducted using a ToF-SIMS IV instrument (IONTOF, GmbH) equipped with a 25 keV Bi$_3$$^+$ liquid metal ion gun (LMIG) and a single-stage reflectron analyzer. A pulsed target current of approximately 0.3 pA and post-acceleration energy of 10 keV were used. The primary ion dose density was maintained at $< 1 \times 10^{12}$ ions per cm^2 to ensure static conditions

and a low energy (< 20 eV) electron flood gun was used for charge compensation of the sample. Spectra were acquired in 'high current bunched' mode in both positive and negative polarity. A 4 × 4 mm area was scanned for each sample; capturing both the spotted material and silicon wafer substrate in each scanned area. These areas were scanned using the macro-raster stage function, with a random raster pattern. A total of 64 separate 0.5 × 0.5 mm patches were scanned, with 15 scans acquired per patch giving a resolution of 100 pixels/mm. The ToF-SIMS data were acquired and analyzed using SurfaceLab 6 software (IONTOF, GmbH). Retrospective analysis allowed a region of interest to be created around the spotted material exclusively, thereby removing data relating to the silicon wafer substrate. This region of interest was then split into four smaller analysis regions, which produced a repeat of n = 4 for every sample. Peak intensities were normalized to the total ion count of the spectra. The fragment ions $C_2H_2O_2^-$ and $C_2H_5O_2^+$ are indicative of PEG.

Protein adsorption: The NPs were diluted 1/100 in either DIW, 8wt% BSA (Sigma Aldrich) or rat serum (Sigma Aldrich) and vortexed. After 30 min, immediately before analysis, the samples were further diluted 100× in DIW and mixed by pipetting. The NP size in the different sera was measured using Nanoparticle Tracking Analysis (NTA, NanoSight LM10, Malvern) with a 488nm laser. For each sample, 3 measurements of 60 seconds were performed and reported numbers are average of the mean size from these 3 measurements.

NP diffusion in *in vitro* ECM model: Collagen gels were made from rat-tail collagen type I high concentration (8-11 mg/mL, Fisher Scientific), following the manufacturer's protocol. In brief, collagen solutions were prepared by mixing 10× PBS (phosphate buffered saline, Sigma-Aldrich),

DIW, 1 M sodium hydroxide, and concentrated collagen on ice (5 mg/mL). The solutions were vortexed and their final pH was adjusted to 7.2 ± 0.2 by addition of 0.1 M sodium hydroxide. NPs were added to the gel solution at a concentration of 120 µg/mL. Collagen-NP solutions were thoroughly vortexed and heated to $37^{\circ}C$ in µ-slide 8-wells imaging plates (Ibidi) for 1 h for polymerization.

Confocal laser scanning images were acquired shortly after the polymerization of the collagen- NP gels and diffusion coefficient analysis was performed using Raster Image Correlation Spectroscopy (RICS). An inverted LSM 510 microscope (Carl Zeiss) was used, with a water immersion objective C- Apochromat *40X/1.2 NA* and a HeNe laser at wavelength 543 nm to excite NR688. Time series of confocal images for diffusion coefficient analysis were obtained by recording consecutive images of the NPs in the gel. For every experiment, 8 or 15 frames at minimum 6 locations in the gel, consisting of 512x512 pixels, were collected. The scan speed along the fast scanning axis was 51.2 µ*s/pixel* and the scan step corresponding to one pixel was 54.9 nm. The diffusion coefficients of the NPs were calculated using the RICS MANICS[22].

Cellular association: Murine leukemia macrophages (RAW264.7) were a generous gift from Prof. Anthonsen, NTNU. The cells were cultured in Dulbecco's Modified Eagle's Medium supplemented with 10 % fetal bovine serum (both from ThermoFisher Scientific). For flow cytometry, the cells were seeded on 12-well plates (Costar) 100,000 cells per well. Upon reaching the log-phase they were incubated with the PBCA NPs at 20 µg/mL in 1 mL of medium for 3 h. Following that, the cells were detached, washed twice with PBS (Sigma) and analyzed using flow cytometry (Gallios, Beckman Coulter). NR688 encapsulated in the NPs were excited at 561 nm

and fluorescence was detected at 620 nm using a 30 nm bandpass filter. The analysis included 10,000 cells; cell debris, dead cells and aggregates were excluded by gating the cell population on a dot plot of forward light scatter signal versus side scatter signal. The uptake of NPs was measured as the median fluorescence intensity relative autofluorescence from the population of untreated cells. To compare the cellular association and uptake of NPs which had different fluorescence intensities, we used a normalization factor. This factor was found by measuring the fluorescence intensity of NPs in PBS using a spectrophotometer (Infinite 200Pro, Tecan).

In vivo **blood circulation half-life:** Circulation half-life of the NPs was determined in female Balb/c nude mice (Envigo). All experimental procedures were approved by the Norwegian Animal Research Authorities. Mice were purchased at 6 weeks of age and housed in specific pathogen free conditions in groups of 4 in individually ventilated cages at temperatures of 22-23°C, 50–60% relative humidity, with *ad libidum* access to food and sterile water. The animals were anesthetized by fentanyl (0.05 mg/kg, Actavis Group hf), medetomidine (0.5 mg/kg, Orion Pharma), midazolam (5 mg/kg, Accord Healthcare Limited), water (2:1:2:5) at a dose of 0.1 ml per 10 g injected subcutaneously. The NPs were diluted to 7 mg/mL in phosphate buffer (0.01 M) and injected intravenously as a bolus of 200 µL through the lateral tail vein. Blood samples of 10-15 µL were drawn from the saphenous vein pre-injection and 10 min, 30 min, 1, 2, 4, 6 and 24 h post injection. Samples were diluted in 40 µL 10 IU/mL heparin and vortexed, before they were centrifuged at 3000 rpm for 7 min. Fluorescence in the supernatant was measured by excitation at 535 nm and detection at 620 nm using a spectrophotometer (Infinite 200Pro, Tecan) and normalized to the weight of blood taken. Monoexponentials ($f(t)=ae^{-bt}$) were fitted to fluorescence intensity vs time curves using SigmaPlot, resulting in circulation half-lives ($t_{1/2}=\ln(2)/b$).

Statistical analysis: Statistics were calculated using Prism 7 (Graphpad Software, Inc), unless otherwise noted, calculating mean, standard deviation (s.d.) and unpaired Student T-tests. P<0.05 was considered statistically significant.

Results

Nanoparticle Synthesis: The synthesized NPs had a Z-average diameter ranging from 90-350 nm and poly dispersity index (PDI) between 0.04-0.32 (Fig. 2a, b). Replacing SDS with PEG-based stabilizers resulted in smaller particles with a ζ-potential closer to zero (Fig. 2c, Table 1). Among the different hetero-brushes (JA/Brij, Kol/Brij and Kol/Plu), PEGylation with two different PEGs in the brush regime, there were no significant differences between the different NPs with regard to size or zeta potential (Fig. 2 and Table 1).
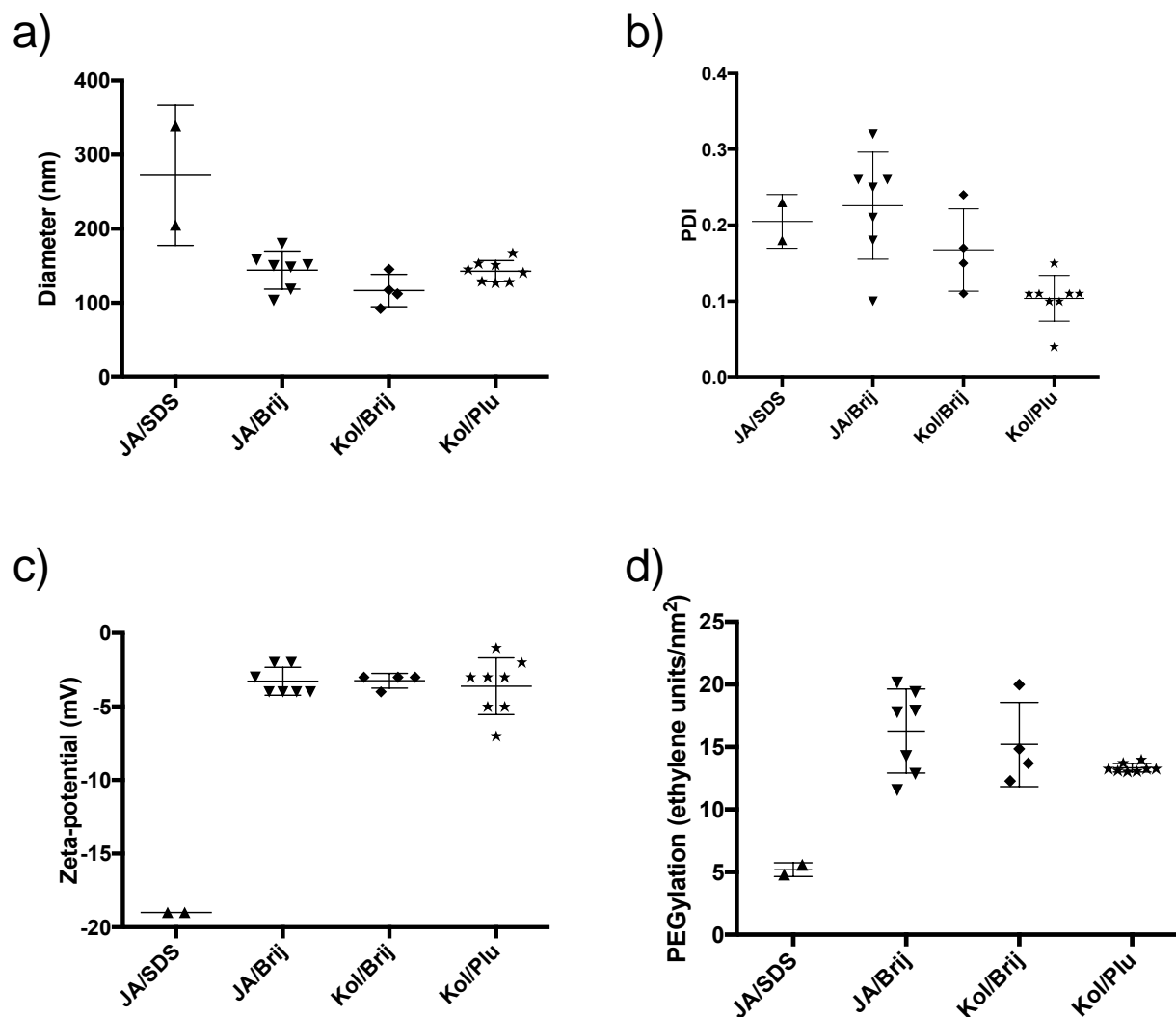
Fig. 2: NP characteristics determined by Dynamic and Electrophoretic Light Scattering (a, b and c) and NMR (d). Each symbol represents a NP batch. Bars are given as mean and s.d.

Quantification of PEG

NMR: ^{1}H-NMR was used to quantify the ethylene glycol units on the NP surface. Data from NMR is summarized in Fig. 2d and in Table 1. NPs with a mixture of JA and SDS were significantly less PEGylated (5.2 ethylene units/nm^2) than NPs with different combinations of PEG-based surfactants (JA/Brij, Kol/Brij or Kol/Plu, 13.3-16.3 ethylene units/nm^2). There was no significant

difference in ethylene unit coverage between the different combinations JA/Brij, Kol/Brij and Kol/Plu and the PEG-density around 15 ethylene units/nm^2 indicates a dense brush confirmation in all three cases.[23] In the set of JA/Brij NPs used in this study only one of seven had JA detectable from the noise level; in that specific case JA constituted only 4.8 mol-% of the total PEG, indicating that the PEGylation of JA/Brij NPs consisted mainly of Brij.

Table 1: PBCA Nanoparticles prepared using various surfactants.

Surfactant	Z-average NP diameter [nm]	PDI	Ethylene units/nm^2	ζ-potential [mV]	# PEG/ nm^2	Number of NP batches analyzed.
Jeffamine M-2070 SDS (JA/SDS)	272 ± 95	0.21 ± 0.035	5.2 ± 0.56	-19 ± 0.00	0.11 ± 0.01	2
Jeffamine M-2070 Brij-L23 (JA/Brij)	144 ± 26	0.23 ± 0.071	16.3 ± 3.4	-3.3 ± 0.95	0.60 ± 0.1	7
Kolliphor HS15 Brij L23 (Kol/Brij)	117 ± 23	0.17 ± 0.054	15.2 ± 3.4	-3.3 ± 0.50	NA	4
Kolliphor HS15 Pluronic F68 (Kol/Plu)	143 ± 14	0.10 ± 0.030	13.3 ± 0.34	-3.6 ±1.9	NA	8

TGA-DSC: A subset of the NPs were analyzed to determine the amount of PEG (wt%) present. Primarily, TG curve as well as its first derivative (DTG) were used to determine the PEG amounts of the analyzed samples The DSC curve and its first derivative (DDSC) were also used as assisting measures for determining the starting and end points of combustion of the different polymeric species. The results can be seen in Table 2.

Table 2. PEG amounts of a subset of nanoparticle samples as determined by TGA-DSC. NA*= value not acquirable

Sample	JA/SDS	JA/Brij	Kol/Brij	Kol/Plu
PEG (wt%)	NA*	14.2	15.6	15.1

Samples JA/Brij, Kol/Brij and Kol/Plu were found to contain between 14 and 16wt% PEG. In JA/SDS neither the TGA or DTGA curve reveals any weight loss step in addition to that of the main big weight loss step of the PACA polymer. The DDSC curve however shows an additional small fluctuation in heat flow at T=245-260°C which could indicate the presence of small amounts of another chemical substance than the PACA polymer itself. It can therefore be assumed that a small amount of PEG was present also on JA/SDS. This value was, however, not acquirable with certainty due to the low quality of the measurement itself. The TGA-DSC measurement curves of all analyzed samples are shown in detail in Supplementary Fig. 3.
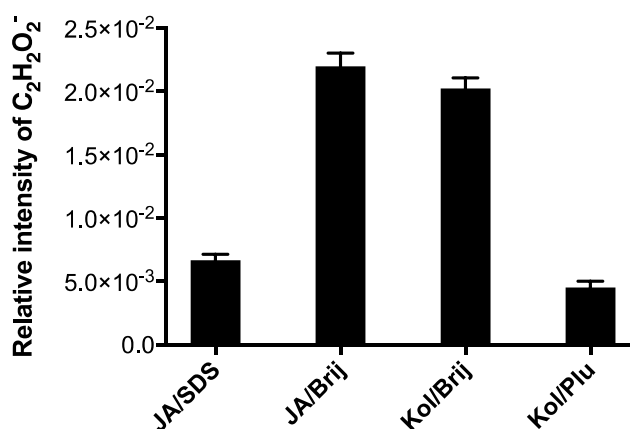

Fig. 3: ToF-SIMS analysis of NPs showing the relative intensities from the PEG fragment $C_2H_2O_2^-$. Number of repeated measurements were 4.

ToF-SIMS: Although ToF-SIMS cannot provide absolute quantification of PEG, it can be used to directly compare PEGylation between different NPs at the surface, as illustrated in Fig. 3. Using

the observed intensity of the $C_2H_2O_2^-$ secondary ion which is indicative of the PEG chemistry, Fig. 3 illustrates a different amount of PEG present at the NP surfaces. The trend in PEGylation between different NPs was independent of the fragment chosen for analysis (Fig. 3, Supplementary Fig. 4a). ToF-SIMS showed the presence of PEG on all particles, but less than expected for Kol/Plu. Increased PEG coverage of the surface of the NP should reduce the amount of PBCA polymer accessible for ToF-SIMS. Analysis of fragments from the PBCA polymer ($C_4H_2NO_2^-$) showed that for JA/SDS, JA/Brij and Kol/Brij the amount of PBCA detected decreased with increasing PEG amount (Fig. 3 and Supplementary Fig. 4b). Interestingly, although having the least amount of PEG-chains on the surface, Kol/Plu also had the least of PBCA on the surface, indicating effective shielding of the particle surface by the long Plu.

Effect of PEGylation on NP properties[*]

To assess how the different PEGylation strategies affect the properties and behavior of NPs, protein adsorption, diffusion in an ECM model, association with macrophages and blood circulation half-life in mice were determined.

Protein adsorption: It is generally considered that the key function of PEG is to hinder protein adsorption to the NP. Serum albumin is the most abundant protein in blood and in rat serum the

---

[*] In the qualitative section a limited set of NPs have been chosen and if the data is correlated to e.g. results from NMR, the NMR data from that specific NP is used in the correlation.

total protein concentration is 4-5% and the albumin concentration is 2-3%.[24] The formation of a protein corona on the PEGylated PBCA particles was indirectly assessed by measuring the immediate size increase of NPs in the presence of 8% BSA, a protein concentration 2-4 times above the one in rat serum. Fig. 4a shows that rat serum resulted in NPs with larger diameter than BSA alone, while in BSA only the JA/Brij NP showed an increase in size. JA/Brij also showed the highest size increase in rat serum. Interestingly, the protein adsorption increased with increasing ethylene units/nm^2 (Fig. 5a). The exact numbers from the NTA measurements are found in Supplementary Table 2 and were in accordance with the DLS measurements.
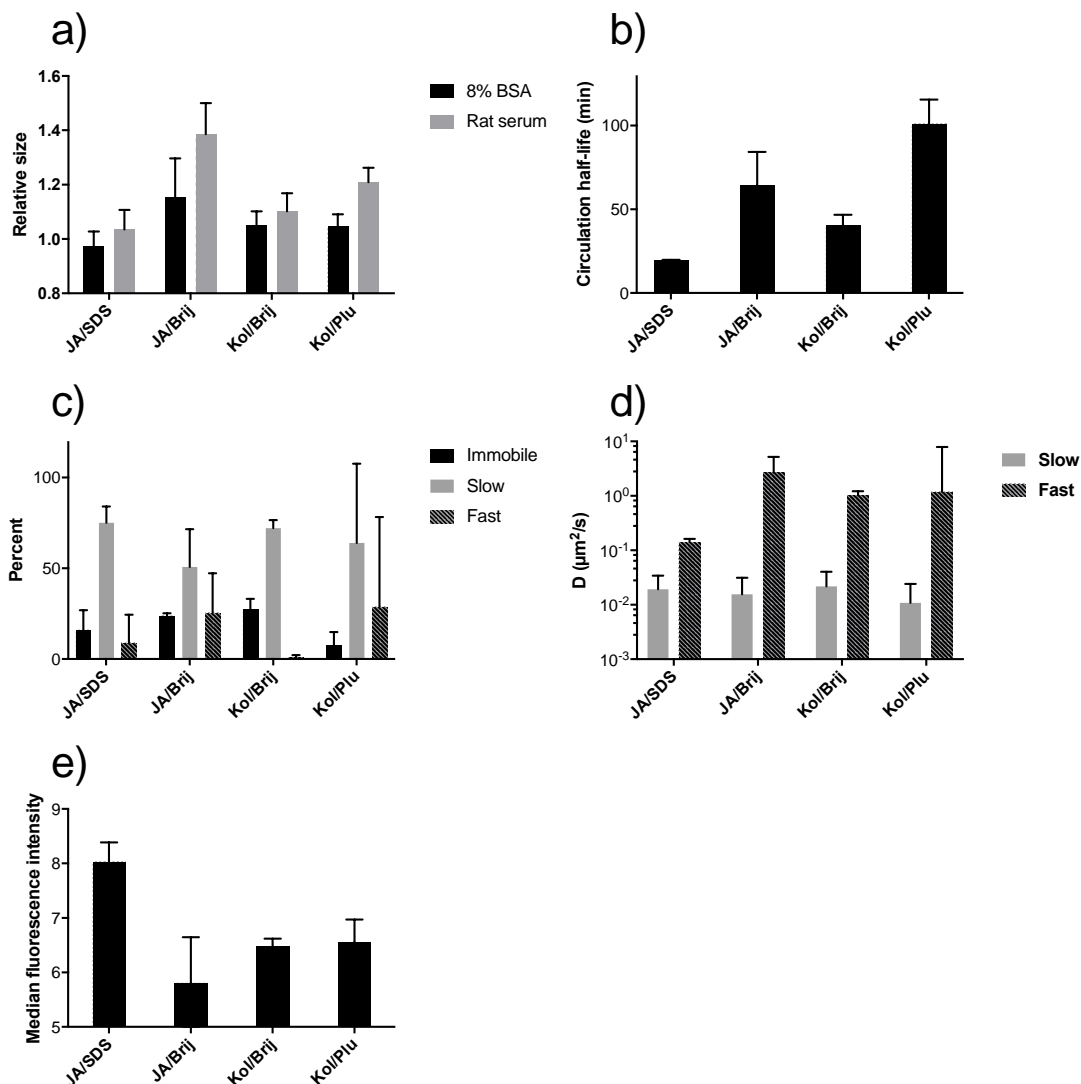
Fig. 4: a) The relative diameter increase of NPs when added to rat serum or 8wt% BSA, compared to PBS, measured by NTA. Number of samples for each NP was 3. b) The circulation half-life of NPs in blood with different PEGylation. Number of samples were 2 (JA/SDS), 4 (JA/Brij), 4 (Kol/Brij), 2 (Kol/Plu). c) NP diffusion, percentage of NPs in each category (immobile, slow or fast). d) Diffusion coefficient for the slow and fast NPs. Number of samples for c) and d) were 3 (JA/SDS), 3 (JA/Brij), 3 (Kol/Brij), 2 (Kol/Plu) e) Normalized median fluorescence intensity from murine macrophages after incubation with NPs. Number of samples for each NP was 3. Error bars are s.d.

Particle diffusion in an *in vitro* ECM model: Once the NP has extravasated from the blood into the ECM, it needs to diffuse further into the tumor to be effective against all tumor cells. The ECM was modeled by a collagen gel, and image analysis of the diffusion of NPs in the gel revealed three

distinct populations of NPs: Fast diffusing, slow diffusing and immobile. The percentage of NP within these groups and their diffusion constants are shown in Fig. 4c and d, respectively. Increased PEGylation resulted in an increased diffusion constant for the fast diffusing NPs (Fig. 5c).

Nanoparticle association with macrophages: *In vivo*, macrophages are crucial for removal of larger debris from circulation, and hence they also target NPs. The interaction of PBCA NPs with macrophages was studied by flow cytometry to measure the amount of fluorescently labeled NPs associated with murine macrophages. The NPs can be both internalized into the cells and bind to the cell surface. As seen in Fig. 4e, the JA/SDS NPs exhibited more association to the macrophages compared to the hetero-brushed NPs. For the latter, no significant difference was observed between the three different combinations. In Fig. 5b it is shown how the interaction with NPs decreased when the PEGylation increased.

***In vivo* blood circulation half-life:** The ultimate purpose of NP PEGylation is to increase the residence time of NPs in circulating blood. Thus, the circulation half-life of PBCA NPs with various PEG layers was measured in mice. As expected, JA/SDS, the NP with the lowest PEG surface coverage, also had the shortest circulation time (Fig. 4b). Further, blood circulation time increased with increasing PEG density (Fig. 5d), except for Kol/Plu, which had the longest residence time in blood even with a lower PEG density than JA/Brij.
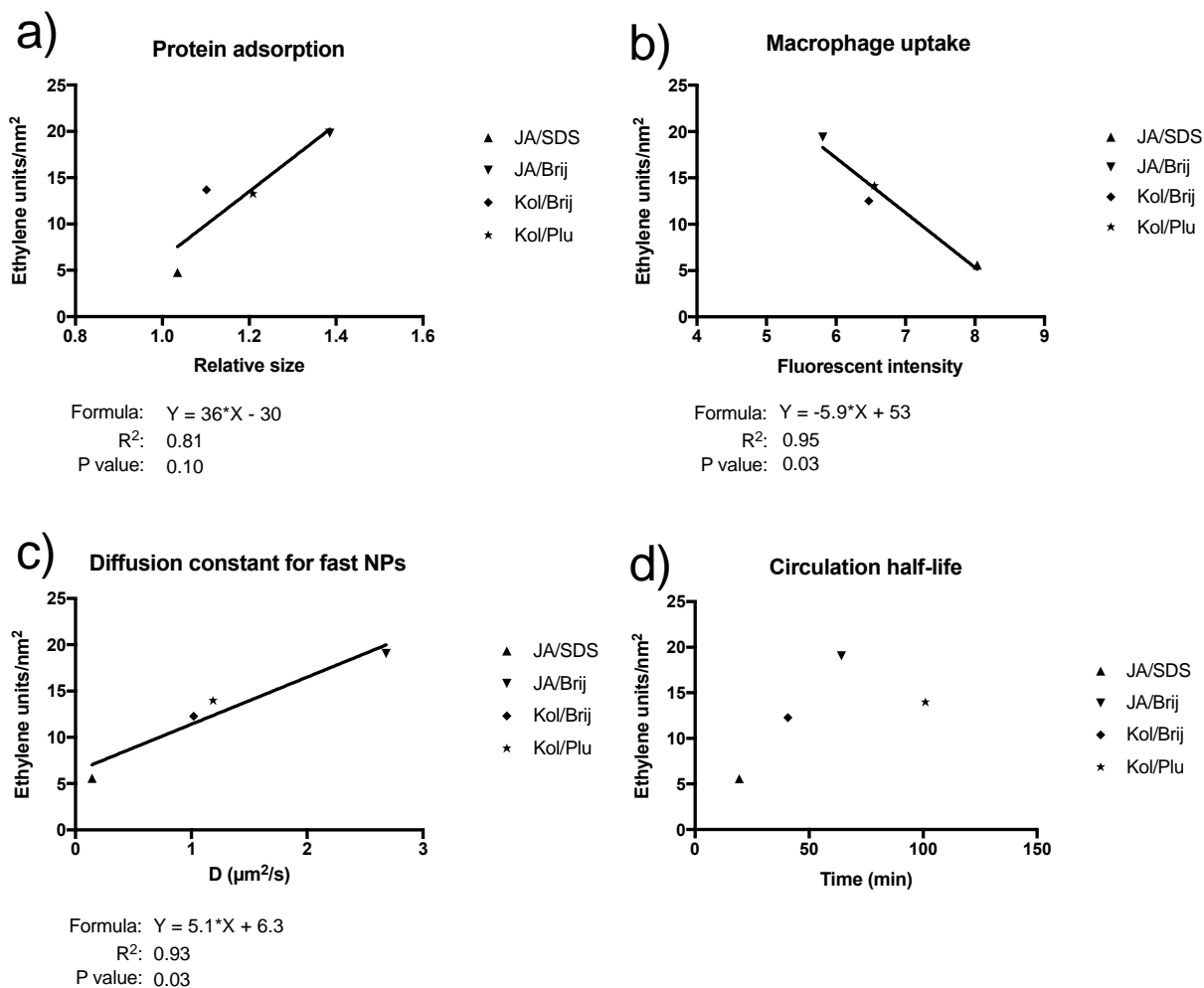
Fig. 5: Correlation between PEGylation measured by NMR and a) protein adsorption, b) macrophage uptake, c) the diffusion constant for fast NPs and d) the blood circulation half-life. All correlations are tabulated with R^2 and P values below the graph.

Discussion

Optimal PEGylation will facilitate a sufficient blood circulation time, high diffusivity in ECM, and low uptake in macrophages. However, there is limited knowledge of optimal PEG-density and PEG chain-length.[25] The physiochemical nature and concentration of stabilizers have been shown

to play an important role on PACA particle size and surface charge.[26] The PEG structures investigated in this study, JA, Brij, Kol and Plu, are composed of a hydrophilic motif, the PEG structure; and a hydrophobic motif, anchoring them to the NP. Although the orientation of these molecules could vary, it is assumed that the PEG structure of the stabilizers (JA, Brij, Kol and Plu) is expressed on the surface of the NP. The hydrophobic end of the stabilizer (hydrocarbon chain or polypropylene glycol) is assumed to be in the shell of the NP. This has previously been confirmed for PLGA and PLA NPs.[27-28] In the specific case of Plu, where the hydrophobic moiety is flanked by two PEG chains, the molecule is expected to be 'u-shaped' so that the two PEG chains extend from the surface. Therefore, every Plu molecule is assumed to contribute with two PEGs extruding from the surface.

Quantification of PEG

In this study, we synthesized four PBCA NPs with different surfactants, Fig. 2 and Table 1 shows that the type of PEG, with and without SDS as a stabilizer, could be conveniently varied. The higher negative charge for SDS NPs is probably caused by the anionic SDS associated to the particle surface. However, hydrolysis of the PBCA butyl esters forming carboxyl groups on the surface of the poorly PEGylated NP surface could also contribute to the negative charges. As anionic surfactants are known to be toxic,[29] the use of non-ionic stabilizers is becoming more prominent within the nanomedicine field. Non-ionic polymeric surfactants have been shown to provide an efficient stabilization against coalescence events because of the steric repulsion they induce between oil droplets.[30] Moreover, the use of mixtures of long and short PEGs on gold surfaces, creating a hetero-brush, have been shown to reduce protein adsorption compared to using

a homogeneous length of PEGs.[31] Replacing SDS with a non-ionic PEG stabilizer reduced the negative charges on the particle surface (ζ-potential from -19 mV with SDS to -3 mV without SDS, Table 1). A slightly negative ζ-potential was measured for NPs with non-ionic PEG-based surfactants, and could be attributed to an increased PEGylation compared to SDS/JA particles, shielding the (partially hydrolyzed) polymer surface of the NP from the surrounding water.

NMR has been used to quantify the PEGylation of polymeric NPs as described previously.[32] Due to few finger print peaks available for different PEGs in NMR, calculating the number of PEG chains/area becomes difficult when a hetero-brush is used. However, in the specific case of JA/Brij, it was possible to calculate the molar ratio of JA and Brij due to the methylene group closest to the amine in JA that can be detected in the NMR spectra (Supplementary Fig. 1), it was found that the NP mainly consisted of Brij. This could be because the hydrophobic component of JA is less hydrophobic than that of Brij and the total free energy of the system is thereby minimized by distribution of Brij on the NP surface and JA dissolved in the water phase. However, as the methylene peak has a low signal-to-noise ratio the values should be interpreted cautiously.

The Flory radius[33] of a PEG is calculated from $R_F = aN^{3/5}$, where a is the monomer length and N is the number of monomers units in the polymer.[23] If the distance (D) between PEG chains is $>2R_F$, the PEGs are not in contact with one another and thus in a mushroom conformation. As the inter-PEG distance reduces, the mushroom conformation is retained, but with possible PEG-PEG steric interactions, until $D<R_F$, where the so-called brush conformation is induced. In the current study, the number of ethylene units/nm^2, calculated by NMR was found to be reasonably constant regardless of the PEG length for the hetero-brushes. Consequently, the total number of PEG

chains/nm^2 is lower when longer PEGs are used compared to shorter PEGs. This reduction in chains/nm^2 is probably due to greater steric hindrance induced by long PEG molecules compared to shorter ones. Therefore, per definition of the Flory radius, the longer PEG with less density on the surface may be further into the brush regime. The Flory radius of JA is ≈7.4 nm, if D=R_F, the PEG coverage would be 0.014 PEG/nm^2, hence even the NP with lowest PEGylation (JA/SDS, 0.1-0.12 PEG/nm^2) have a dense enough packing to be in the brush regime. The PEG coverage was calculated using the Z-average, this will invariably introduce an uncertainty in the coverage, especially for the NPs with high PDI.

ToF-SIMS is beneficial compared to NMR due to the quantification of surface associated material only. As the NPs used in this study are prepared with a combination of different PEGs, a direct comparison to NMR is challenging as the output from NMR is *number of ethylene units* while for ToF-SIMS the output is *number of PEG-chains*. Furthermore, detection of the different PEGs by ToF-SIMS may vary as the end group chemistry of the different PEGs used herein is not identical. Interestingly, the number of PEG chains on the Kol/Plu NP determined by ToF-SIMS was very low. This corroborates with the Flory radius discussion *vide supra*, which indicates that few long chained PEGs may be preferable to many short chained PEGs. Furthermore, if the Kol/Plu NPs were sparsely covered by PEG, it would be shown in an increased signal from the analysis of PBCA polymer fragments. However, the low abundance of both PEG and polymer fragments is an indication that the long Plu will efficiently cover the surface, although being relatively scarce.

TGA was introduced in the study to examine whether it could be used to separately quantify the different PEGs on the hetero-brush NPs due to different combustion temperatures. However, while TGA indicated the presence of PEG at approximately 15%wt for the three mixed-PEG NPs, we were not able to distinguish different PEGs with this method.

Qualitative effects of PEGylation

The formation of a protein corona will occur immediately as the NPs enter the blood. It has been shown that coverage by specific proteins (opsonins) is involved in removal of NPs by the mononuclear phagocyte system (MPS).[10] However, certain proteins can also be part of shielding the NPs and contribute to increasing the circulation time.[34] Consequently, increased circulation time is not solely governed by their ability to reduce protein adsorption to the NP, but also, by which specific proteins that are adsorbed. However, it should be expected that the hydrophilic milieu formed by the PEG layer will reduce non-specific binding occurring on hydrophobic surfaces.[35] Rodent blood serum contains 2-3wt% serum albumin and a total protein concentration of 4-5wt%.[36] If serum albumin has high affinity for the PEGylated surface, a greater increase in size would be expected when mixing the NPs with 8% BSA compared to serum. Our results show that in 8% BSA, there is no size increase for any NPs, except for JA/Brij NPs. However, when the NPs are placed in rat serum all NPs grow except of JA/SDS NPs (Fig. 4a) and the growth of JA/Brij NPs is larger than compared to 8wt% BSA. Hence, it seems that there are other proteins present in blood serum with a higher affinity for the NP surface than serum albumin. In fact, those proteins may play an important role for keeping the NPs in blood circulation, as increased protein adsorption does not directly correlate with reduced blood circulation half-life.

Extracellular matrix consists of a network of collagen fibers embedded in a hydrophilic gel of glysosaminoglycans. Thus we mimicked the extracellular matrix by a gel of collagen fibers. The NPs showed immobile, slow or fast diffusion rates in the collagen gels. This can be explained by

the two-phase nature of transport in the tumor matrix.[37-38] It is likely that the fast component of diffusion is related to the NPs diffusing in aqueous pockets between collagen fibers, thereby the diffusion coefficient is approaching the diffusion coefficient in pure solution.[38] The immobile NPs indicate electrostatic or other interactions between the NP and the collagen fibers. The difference in diffusion coefficients within a phase (fast, slow, immobile) is not statistically significant, and the fraction of NPs in each phase could be a more relevant comparison of the diffusivity between NPs. The NPs in the fast regime correlated with the PEGylation, the more ethylene units/nm^2 the faster the diffusion constant, as previously observed.[39] However, Kol/Brij NPs, with short and dense PEG-layer, had almost no NPs in the fast diffusing regime indicating that the PEG chain length also influences NP diffusion. The fraction of NPs present in each phase could be affected not only by the NP PEGylation, but also by the collagen polymerization, which varied between samples. The collagen volume fraction and fiber size did qualitatively vary between samples and would affect the available aqueous pocket volume and hence the fraction of fast diffusing NPs.

Fast uptake of NPs by macrophages significantly reduces the residence time of NPs in the blood stream, also reducing their efficacy. To model the uptake by the MPS system, the NPs were incubated with RAW264.7 murine macrophages (Fig. 4e). It was observed that hetero-brush NPs had a moderate but significantly reduced association to the macrophages compared to the NPs stabilized by JA/SDS. The JA/SDS NPs are both larger and more negatively charged which both have previously been to alter the association of NPs to cells.[40-41] As the association to cells is still higher for these NPs (Fig. 5b), we hypothesize that steric hindrance by PEG is superior to anionic repulsion for avoiding cell contact. Similar trends have previously been reported for chitosan NPs.[40] As the NP association with RAW264.7 was measured by flow cytometry, surface bound

NPs cannot be distinguished from internalized material. However, in a previous study, we found that Brij coated PBCA NPs were endocytosed, whereas very limited surface binding was observed.[42] Our results suggest that dense PEGylation can reduce the uptake by MPS, similarly to what we have previously shown in rat brain endothelial cells[43] and compliance with other studies.[44]

The blood circulation half-life of the NPs in mice varied significantly depending on the types of stabilizers used (Fig. 4b and 5d). JA/SDS NPs (the least PEGylated NP) had a half-life of 20 min, whereas for Kol/Plu NPs it was extended by five times to 100 min. Between JA/SDS, JA/Brij and Kol/Brij NPs there seems to be a correlation indicating that increased amount of ethylene units/nm^2 increases the circulation time (Fig 5d). Kol/Plu NPs stand out by having fever ethylene units/nm^2, but still having the longest circulation half-life. This might be due to Plu having a considerably longer PEG chain compared to Kol, Brij and JA and therefore creating a thicker brush that protects the NPs from opsonization and clearance from the blood. Similarly the chain length difference between JA, Brij and Kol is not that large, and the amount of ethylene units/nm^2 may be a good approximation for their different coverage.

The reports on PEGylated PACA NPs and their circulation time are very limited.[15, 45] In line with our findings, Fang et al. found that when the coverage and size of poly(methoxypolyethyleneglycol cyanoacrylate-co-*n*-hexadecyl cyanoacrylate) NPs remained consistent, longer PEGs increased the circulation half-life.[15] Also, they found that when the PEG chain length was kept constant and the size of the NP was varied, bigger NPs tended to circulate a shorter time than smaller ones. In our case, the SDS NPs were different to other NPs in terms of size and ζ-potential (Fig. 2a and b),

hence it is possible that these properties are partly responsible for the short circulation time of this NP. For the other NPs, the differences can be explained neither by size nor by ζ-potential.

The JA/SDS NP, with significanly less PEG than the other NPs, was efficiently shielded against protein association, but still showed increased association with macrophages. JA/SDS NPs also diffuse considerably shorter in collagen gels and have the shortest blood circulation time in mice. The decreased diffusivity, and possibly also the circulation time, might be attributed to the size of these NPs, having almost twice the radii of the hetero-brush NPs. However, from the Stokes-Einstein equation, the diffusion coefficient is proportional to $1/r$, while almost a 10-fold decrease in diffusion is observed instead of half as expected from the size increase, demonstarting the importance on optimal PEGylation. Comparing Kol/Brij to Kol/Plu, it was found that the longer, less densely packed, PEG chain of Plu is favorable, especially in terms of circulation half-life, but also indicated by lower protein absorption and association with macrophages.

Conclusion

To progress in the field of NP mediated drug delivery, the interaction between NPs and biological fluids must be better understood, and PEG stands as the key player in this interaction. To do so quantitative and semi-quantitative measurements of PEGylated NPs we compared by NMR, TGA and ToF-SIMS. Our results show that NMR is the most direct and precise method of quantification, offering absolute quantification. However, distinguishing between associated and unassociated PEG can be a challenge. The use of NMR for quantifying combinations of PEG is also limiting when no fingerprint signals are available for the different PEGs. ToF-SIMS, although not quantitative, analyzes PEG on the NP surface and 'counts' the molar amount of PEG. It indicates how well the surface of the NP is shielded by the PEGylation when the polymer fragment is

analyzed, and is thereby a valuable complement to NMR. TGA could not contribute with more precise measurements than the other methods in this study.

The qualititative assessment of the PEGylation draws a comprehensive, but not fully coherent picture. Not only PEG density, but also the PEG chain length affects the NP properties. We found that increasing PEG density does not necessarily correlate with decreasing protein adsorption, and further that protein adsorption not directly correlates with reduced blood circulation half-life. The NP diffusivity in a collagen gel was affected by PEG density, and can hence give an indication on the effectiveness of PEGylation. Furthermore, a negative correlation between PEG density and NP uptake by macrophages was observed, while the circulation half-life was influences by both PEG density and PEG chain length. Both methods are useful for predicting PEGylation efficiency.

This study has illustrated that no single method can give a comprehensive picture of neither PEG amount nor effects of PEGylation on NP properties. In order to understand how PEGylation affects NP properties and their behaviour in biological settings, complementary techniques, both quantitative and qualitative, are needed. The best suited methods have to be evaluated in each setting, depending on the type of particle and PEG material.

References

1.   Tibbitt, M. W.; Dahlman, J. E.; Langer, R., Emerging Frontiers in Drug Delivery. *Journal of the American Chemical Society* **2016,** *138* (3), 704-17.

2.   Bae, Y. H., Drug targeting and tumor heterogeneity. *J. Control Release* **2009,** *133* (1), 2-3.

3.   Yuan, F.; Leunig, M.; Huang, S. K.; Berk, D. A.; Papahadjopoulos, D.; Jain, R. K., Microvascular permeability and interstitial penetration of sterically stabilized (stealth) liposomes in a human tumor xenograft. *Cancer research* **1994,** *54* (13), 3352-6.

4.   Schiffelers, R. M.; Banciu, M.; Metselaar, J. M.; Storm, G., Therapeutic application of long-circulating liposomal glucocorticoids in auto-immune diseases and cancer. *J. Liposome Res.* **2006,** *16* (3), 185-94.

5.   Åslund, A. K. O.; Berg, S.; Hak, S.; Morch, Y.; Torp, S. H.; Sandvig, A.; Wideroe, M.; Hansen, R.; Davies, C. d. L., Nanoparticle delivery to the brain - By focused ultrasound and self-assembled nanoparticle-stabilized microbubbles. *Journal of Controlled Release* **2015,** *220*, 287-294.

6.   Hak, S.; Helgesen, E.; Hektoen, H. H.; Huuse, E. M.; Jarzyna, P. A.; Mulder, W. J.; Haraldseth, O.; Davies Cde, L., The effect of nanoparticle polyethylene glycol surface density on ligand-directed tumor targeting studied in vivo by dual modality imaging. *ACS nano* **2012,** *6* (6), 5648-58.

7.   Maeda, H., Toward a full understanding of the EPR effect in primary and metastatic tumors as well as issues related to its heterogeneity. *Adv Drug Deliver Rev* **2015,** *91*, 3-6.

8.   Cheng, C. J.; Tietjen, G. T.; Saucier-Sawyer, J. K.; Saltzman, W. M., A holistic approach to targeting disease with polymeric nanoparticles. *Nature reviews. Drug discovery* **2015,** *14* (4), 239-47.

9.   Swenson, C. E.; Haemmerich, D.; Maul, D. H.; Knox, B.; Ehrhart, N.; Reed, R. A., Increased Duration of Heating Boosts Local Drug Deposition during Radiofrequency Ablation in Combination with Thermally Sensitive Liposomes (ThermoDox) in a Porcine Model. *PloS one* **2015,** *10* (10), e0139752.

10.   Alexis, F.; Pridgen, E.; Molnar, L. K.; Farokhzad, O. C., Factors affecting the clearance and biodistribution of polymeric nanoparticles. *Mol Pharm* **2008,** *5* (4), 505-15.

11.   Harris, J. M.; Chess, R. B., Effect of pegylation on pharmaceuticals. *Nature reviews. Drug discovery* **2003,** *2* (3), 214-21.

12.   Georgiev, G. A.; Sarker, D. K.; Al-Hanbali, O.; Georgiev, G. D.; Lalchev, Z., Effects of poly (ethylene glycol) chains conformational transition on the properties of mixed DMPC/DMPE-PEG thin liquid films and monolayers. *Colloids Surf B Biointerfaces* **2007,** *59* (2), 184-93.

13.   Kumari, A.; Yadav, S. K.; Yadav, S. C., Biodegradable polymeric nanoparticles based drug delivery systems. *Colloids Surf B Biointerfaces* **2010,** *75* (1), 1-18.

14.   Vauthier, C.; Dubernet, C.; Fattal, E.; Pinto-Alphandary, H.; Couvreur, P., Poly(alkylcyanoacrylates) as biodegradable materials for biomedical applications. *Adv Drug Deliv Rev* **2003,** *55* (4), 519-48.

15.   Fang, C.; Shi, B.; Pei, Y. Y.; Hong, M. H.; Wu, J.; Chen, H. Z., In vivo tumor targeting of tumor necrosis factor-alpha-loaded stealth nanoparticles: effect of MePEG molecular weight and particle size. *Eur J Pharm Sci* **2006,** *27* (1), 27-36.

16.   Mørch, Ý.; Hansen, R.; Berg, S.; Åslund, A. K. O.; Glomm, W. R.; Eggen, S.; Schmid, R.; Johnsen, H.; Kubowicz, S.; Snipstad, S.; Sulheim, E.; Singh, G.; McDonagh, B. H.; Blom, H.; Davies, C. d. L.; Stenstad, P. M., Nanoparticle-Stabilized Microbubbles for Multimodal Imaging and Drug Delivery. *Contrast Media Mol. Imaging* **2015,** *10* (5), 356-66.

17.   Klymchenko, A. S.; Roger, E.; Anton, N.; Anton, H.; Shulov, I.; Vermot, J.; Mely, Y.; Vandamme, T. F., Highly lipophilic fluorescent dyes in nano-emulsions: towards bright non-leaking nano-droplets. *Rsc Adv* **2012,** *2* (31), 11876-11886.

18.   Snipstad, S.; Hak, S.; Baghirov, H.; Sulheim, E.; Morch, Y.; Lelu, S.; von Haartman, E.; Back, M.; Nilsson, K. P.; Klymchenko, A. S.; de Lange Davies, C.; Aslund, A. K. O., Labeling nanoparticles: Dye leakage and altered cellular uptake. *Cytometry A* **2016**.

19.   Gottlieb, H. E.; Kotlyar, V.; Nudelman, A., NMR Chemical Shifts of Common Laboratory Solvents as Trace Impurities. *The Journal of organic chemistry* **1997,** *62* (21), 7512-7515.

20.   Langer, K.; Seegmuller, E.; Zimmer, A.; Kreuter, J., Characterization of Polybutylcyanoacrylate Nanoparticles .1. Quantification of Pbca Polymer and Dextrans. *International Journal of Pharmaceutics* **1994,** *110* (1), 21-27.

21.   Bootz, A.; Vogel, V.; Schubert, D.; Kreuter, J., Comparison of scanning electron microscopy, dynamic light scattering and analytical ultracentrifugation for the sizing of poly(butyl cyanoacrylate) nanoparticles. *European journal of pharmaceutics and biopharmaceutics : official journal of Arbeitsgemeinschaft fur Pharmazeutische Verfahrenstechnik e.V* **2004,** *57* (2), 369-75.

22.   Hamrang, Z.; Pluen, A.; Zindy, E.; Clarke, D., Raster image correlation spectroscopy as a novel tool for the quantitative assessment of protein diffusional behaviour in solution. *Journal of pharmaceutical sciences* **2012,** *101* (6), 2082-93.

23.   Nicholas, A. R.; Scott, M. J.; Kennedy, N. I.; Jones, M. N., Effect of grafted polyethylene glycol (PEG) on the size, encapsulation efficiency and permeability of vesicles. *Bba-Biomembranes* **2000,** *1463* (1), 167-178.

24.   Zaias, J.; Mineau, M.; Cray, C.; Yoon, D.; Altman, N. H., Reference values for serum proteins of common laboratory rodent strains. *J Am Assoc Lab Anim Sci* **2009,** *48* (4), 387-90.

25.   Rabanel, J.-M.; Hildgen, P.; Banquy, X., Assessment of PEG on Polymeric Particles Surface, a Key Step in Drug Carrier Translation. *Journal of Controlled Release* **2014,** *185*, 71-87.

26.   Douglas, S. J.; Illum, L.; Davis, S. S.; Kreuter, J., Particle-Size and Size Distribution of Poly(Butyl-2-Cyanoacrylate) Nanoparticles .1. Influence of Physicochemical Factors. *Journal of colloid and interface science* **1984,** *101* (1), 149-158.

27.   Hrkach, J. S.; Peracchia, M. T.; Domb, A.; Lotan, N.; Langer, R., Nanotechnology for biomaterials engineering: structural characterization of amphiphilic polymeric nanoparticles by 1H NMR spectroscopy. *Biomaterials* **1997,** *18* (1), 27-30.

28.   Rabanel, J. M.; Faivre, J.; Tehrani, S. F.; Lalloz, A.; Hildgen, P.; Banquy, X., Effect of the Polymer Architecture on the Structural and Biophysical Properties of PEG-PLA Nanoparticles. *ACS applied materials & interfaces* **2015,** *7* (19), 10374-85.

29.   Sirisattha, S.; Momose, Y.; Kitagawa, E.; Iwahashi, H., Toxicity of anionic detergents determined by Saccharomyces cerevisiae microarray analysis. *Water Res* **2004,** *38* (1), 61-70.

30.   Durand, A.; Marie, E., Macromolecular surfactants for miniemulsion polymerization. *Adv Colloid Interfac* **2009,** *150* (2), 90-105.

31.   Uchida, K.; Otsuka, H.; Kaneko, M.; Kataoka, K.; Nagasaki, Y., A reactive poly(ethylene glycol) layer to achieve specific surface plasmon resonance sensing with a high S/N ratio: the substantial role of a short underbrushed PEG layer in minimizing nonspecific adsorption. *Anal Chem* **2005,** *77* (4), 1075-80.

32.   Nance, E. A.; Woodworth, G. F.; Sailor, K. A.; Shih, T. Y.; Xu, Q.; Swaminathan, G.; Xiang, D.; Eberhart, C.; Hanes, J., A dense poly(ethylene glycol) coating improves penetration of large polymeric nanoparticles within brain tissue. *Science translational medicine* **2012,** *4* (149), 149ra119.

33.   de Gennes, P. G., Polymers at an interface; a simplified view. *Adv Colloid Interfac* **1987,** *27* (3), 189-209.

34.   Schottler, S.; Becker, G.; Winzen, S.; Steinbach, T.; Mohr, K.; Landfester, K.; Mailander, V.; Wurm, F. R., Protein adsorption is required for stealth effect of poly(ethylene glycol)- and poly(phosphoester)-coated nanocarriers. *Nat Nanotechnol* **2016,** *11* (4), 372-377.

35.   Roach, P.; Farrar, D.; Perry, C. C., Interpretation of protein adsorption: surface-induced conformational changes. *Journal of the American Chemical Society* **2005,** *127* (22), 8168-73.

36.   Shen, Y. F.; Jacobs, J. M.; Camp, D. G.; Fang, R. H.; Moore, R. J.; Smith, R. D.; Xiao, W. Z.; Davis, R. W.; Tompkins, R. G., Ultra-high-efficiency strong cation exchange LC/RPLC/MS/MS for high dynamic range characterization of the human plasma proteome. *Analytical Chemistry* **2004,** *76* (4), 1134-1144.

37.   Alexandrakis, G.; Brown, E. B.; Tong, R. T.; McKee, T. D.; Campbell, R. B.; Boucher, Y.; Jain, R. K., Two-photon fluorescence correlation microscopy reveals the two-phase nature of transport in tumors. *Nature medicine* **2004,** *10* (2), 203-7.

38.   Chauhan, V. P.; Lanning, R. M.; Diop-Frimpong, B.; Mok, W.; Brown, E. B.; Padera, T. P.; Boucher, Y.; Jain, R. K., Multiscale measurements distinguish cellular and interstitial hindrances to diffusion in vivo. *Biophysical journal* **2009,** *97* (1), 330-6.

39.   Lelu, S.; Strand, S. P.; Steine, J.; Davies Cde, L., Effect of PEGylation on the diffusion and stability of chitosan-DNA polyplexes in collagen gels. *Biomacromolecules* **2011,** *12* (10), 3656-65.

40.   He, C.; Hu, Y.; Yin, L.; Tang, C.; Yin, C., Effects of particle size and surface charge on cellular uptake and biodistribution of polymeric nanoparticles. *Biomaterials* **2010,** *31* (13), 3657-66.

41.   dos Santos, T.; Varela, J.; Lynch, I.; Salvati, A.; Dawson, K. A., Quantitative assessment of the comparative nanoparticle-uptake efficiency of a range of cell lines. *Small* **2011,** *7* (23), 3341-9.

42.   Sulheim, E.; Baghirov, H.; von Haartman, E.; Boe, A.; Åslund, A. K. O.; Morch, Y.; Davies Cde, L., Cellular uptake and intracellular degradation of poly(alkyl cyanoacrylate) nanoparticles. *J Nanobiotechnology* **2016,** *14* (1), 1.

43.   Baghirov, H.; Melikishvili, S.; Mørch, Y.; Sulheim, E.; Åslund, A. K.; Hianik, T.; de Lange Davies, C., The effect of poly(ethylene glycol) coating and monomer type on poly(alkyl cyanoacrylate) nanoparticle interactions with lipid monolayers and cells. *Colloids Surf B Biointerfaces* **2016**.

44.   Chaudhari, K. R.; Ukawala, M.; Manjappa, A. S.; Kumar, A.; Mundada, P. K.; Mishra, A. K.; Mathur, R.; Monkkonen, J.; Murthy, R. S., Opsonization, biodistribution, cellular uptake and apoptosis study of PEGylated PBCA nanoparticle as potential drug delivery carrier. *Pharmaceutical research* **2012,** *29* (1), 53-68.

45.   Reddy, L. H.; Murthy, R. S., Pharmacokinetics and biodistribution studies of Doxorubicin loaded poly(butyl cyanoacrylate) nanoparticles synthesized by two different techniques. *Biomed Pap Med Fac Univ Palacky Olomouc Czech Repub* **2004,** *148* (2), 161-6.